Earthquakes and Structures, *Vol. 10, No. 6 (2016) 1467-1486*
DOI: http://dx.doi.org/10.12989/eas.2016.10.6.1467

Seismic performance of single pier skewed bridges with different pier-deck connections

Nahid Attarchian[a], Afshin Kalantari[*] and Abdolreza S. Moghadam[b]

Int'l Institute of Earthquake Eng. and Seismology (IIEES), No. 21, Arghavan St., North Dibajee, Farmanieh, Tehran, Iran

(Received February 14, 2015, Revised March 5, 2016, Accepted May 23, 2016)

Abstract. This research focuses on seismic performance of a class of single pier skewed bridges with three different pier-deck connections; skew angles vary from 0° to 60°. A well-documented four span continuous deck bridge has been modeled and verified. Seat-type connections with fixed and sliding bearings plus monolithic pier-deck connections are studied. Shear keys are considered either fully operational or ineffective. Seismic performances of the bridges and the structural components are investigated conducting bidirectional nonlinear time history analysis in OpenSees. Several global and intermediate engineering demand parameters (EDP) have been studied. On the basis of results, the values of demand parameters of skewed bridges, such as displacement and rotation of the deck plus plastic deformation and torsional demand of the piers, increase as the skew angle increases. In order to eliminate the deck collapse probability, the threshold skew angle is considered as 30° in seat-type bridges. For bridges with skew angles greater than 30°, monolithic pier-deck connections should be applied. The functionality of shear keys is critical in preventing large displacements in the bearings. Pinned piers experience considerable ductility demand at the bottom.

Keywords: skewed bridge; pier-deck connection; single pier; nonlinear time history; combined loading; torsion; fixed bearing; sliding bearing; shear key

1. Introduction

According to the observations of recent earthquakes, the responses of straight bridges are significantly different from those of skewed bridges (Elnashai *et al*. 2010, Zhao and Taucer 2010, Yen *et al*. 2011a). Common behavior mode in seat-type skewed bridges is composed of transversal and longitudinal movements plus rotation about the vertical axis of the deck. This fact may lead to deck collapse or considerable residual displacements in the bearings, Fig. 1. On the other hand, extensive damage is probable in the substructure of skewed bridges with monolithic pier-deck connections, Fig. 2. Therefore, design parameters must be determined properly since functionality of bridges after an earthquake is essential. In the design process of bridges, some characteristics

*Corresponding author, Assistant Professor, E-mail: a.kalantari@iiees.ac.ir
[a]Ph.D. Student, E-mail: n.attarchian@iiees.ac.ir
[b]Associate Professor, E-mail: moghadam@iiees.ac.ir

http://www.techno-press.com/journals/eas&subpage=7 ISSN: 2092-7614 (Print), 2092-7622 (Online)

like the whole length of the bridge, skew angle or curvature of the plan are predetermined. However, the parameters such as structural system, pier and deck section types and connections can be adjusted and assigned by the designer. Priestley *et al*. (2007) have presented general characteristics and qualitative description of two main classes of pier-deck connections (monolithic and seat-type). However, so far no guideline is available to determine pier-deck connections based on the skew angle in the skewed bridges.

Several studies mainly concentrated on the seismic performance of bridges (Olmos and Roesset 2010, Bhagwat *et al.* 2011 and Ramanathan *et al.* 2015). There, it has been concerned about analytical/numerical modeling of bridge components and the validity of models in capturing peculiar collapse mechanisms of skewed bridges under seismic excitations. Ghobarah and Tso (1974) used spine-line model to represent bridge deck and columns. They concluded that the bridge collapse was due to the coupled flexural-torsional motions of the bridge deck or excessive compression demands that resulted in column failures. Meng and Lui (2000) investigated the behavior of Foothill Boulevard Undercrossing and proposed that seismic response of a bridge is strongly influenced by column boundary conditions and skew angle. Ijima *et al*. (2001) developed an analytical model to investigate deck movements in the skewed and curved bridges. They found that, reducing the clearance between deck and abutments is the most effective approach for decreasing the deformations as well as the damage caused by collision. Consequently, abutments should be designed for the force caused by elongated deck in the high temperature. In a more recent study, Mohti and Peckan (2008) assessed the seismic performance of a three-span continuous box girder bridge for skew angle of 0-60°. They compared finite element and beam-stick modeling approaches. Based on their studies, coupled lateral-torsional response of moderate skewed bridges could be captured via simplified beam-stick models. An approximate method for dynamic analysis of skewed highway bridges with continuous rigid deck is proposed by Kalantari and Amjadian (2010). The preliminary values of this method can help to identify the unknown errors occurring during finite element modeling of the structural model. Kaviani *et al*. (2012) investigated the seismic behavior of a group of short reinforced concrete bridges with seat-type abutments in California and proposed an approach for modeling skew-angled seat-type abutments. They showed that, bridges with larger abutment skew angles bear a higher probability of collapse due to excessive rotations. Besides, the shear keys can play a major role in reducing deck rotations and thus the probability of collapse. The aforementioned studies have resulted in a better understanding of seismic behavior of skewed bridges. However, comparing the behavior of skewed bridges with regards to different pier-deck connections has yet to be addressed.

The main objective of this research is to determine the superiority of investigated connections upon different skew angles, considering the criteria of: a) eliminating the possibility of deck collapse; b) restricting the demand in substructure elements. Furthermore, the existence of any threshold skew angle which can affect the connection choices in single pier skewed bridges will be investigated.

In this study, a well-documented four span continuous deck bridge with single pier bents is modeled; the skew angles vary from 0° to 60°. Three different types of pier-deck connections are applied in the considered skew angles. The numerical spine models are developed in OpenSees (2008). The soil-structure interaction in foundations and the interaction between abutment and bridge are ignored in order to determine the pure influence of varying parameters a) different pier-deck connections and b) skew angles. The models have been subjected to the bidirectional earthquake excitations. Their seismic performances have been investigated through nonlinear time history analysis. The trends in seismic responses are studied considering different skew angles and

(a)

(b)

Fig. 1 Failures in seat-type skewed bridges: (a) 1.8 m transverse displacement in 80° skewed bridge, Mingjiang Bridge, China 2008 (Zhiqiang and Lee 2009); (b) Deck rotation from obtuse corner toward acute corner and span collapse in 40° skewed bridge (Yen *et al.* 2011b)

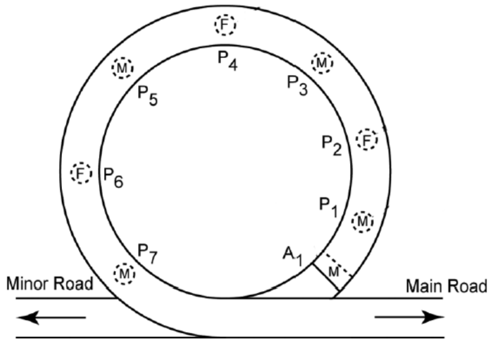

(a)

(b)

Fig. 2 Shear and flexural failures in fixed pier of Huilan bridge: (a) bridge plan (F: fixed connection, M: rubber bearing); (b) damaged fixed P4 (left), undamaged pinned P3 (right) (Kawashima *et al.* 2009)

connection types. Several global and intermediate engineering demand parameters (EDP) are selected in order to compare the overall behavior of the bridges, plus the performance of structural components. Investigated EDPs are displacement and rotation in the deck, hysteresis behavior of plastic hinges of the piers, deformation ductility and forces in the piers, plus bearings and connections.

2. Characteristics of the reference multi span bridge

Multicolumn bent bridges provide relatively larger global torsional stiffness in comparison to single column bent bridges. Consequently, they are better choices for skewed bridges. However, in this research a four span continuous deck bridge with single pier bents has been chosen as the seed bridge in order to investigate a more critical case. The structure has been designed according to

Eurocode 8 provisions (CEN 2002) for PGA 0.35 g (Pinto *et al*. 1996). It is a well- documented bridge, widely applied by the researchers (Kappos *et al*. 2002, Isakovi´C *et al*. 2008). Fig. 3 shows the plan, elevation, global axes, and local longitudinal and transversal axes of the bridge. The overall dimensions and cross section details of the deck and piers are shown in Fig. 4. Longitudinal reinforcement ratio for all pier sections is considered constant (0.515%). Applying similar pier design in all models may not realistically represent the actual design practice. In order to compare the results, the identical samples are selected in such a way to be different only in the connection types and skew angles. The abutments are seat-type with bearings under the webs of box girder; and the piers are supported on spread footings. The properties of concrete are selected in accordance with C25/30 and all reinforcing bars are S500.

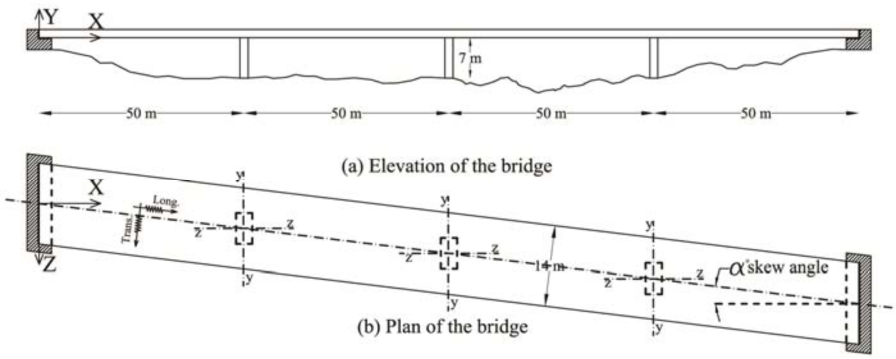

Fig. 3 General layout of the benchmark Bridge

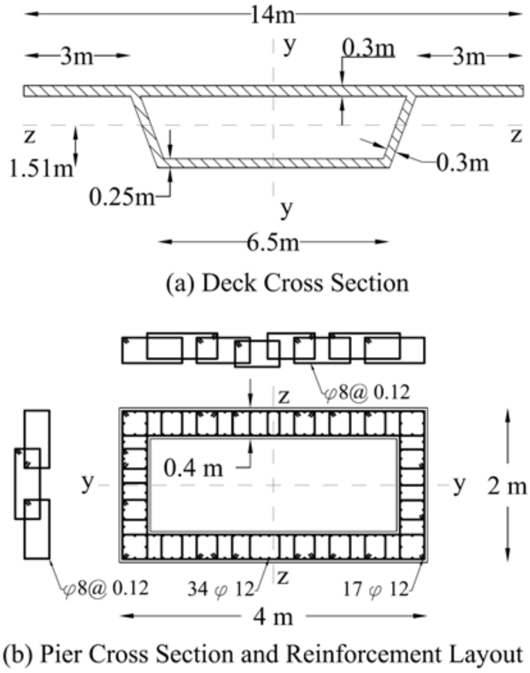

Fig. 4 Cross sections of deck and piers

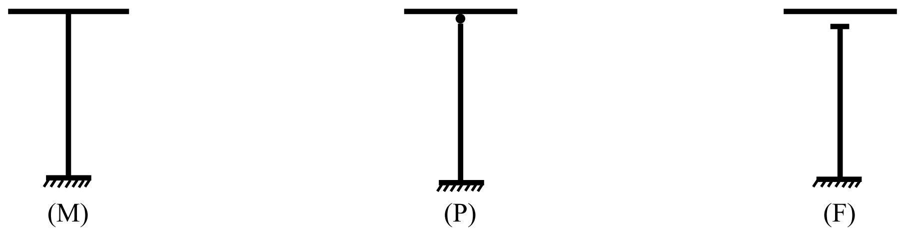

Fig. 5 The schematic description of the models

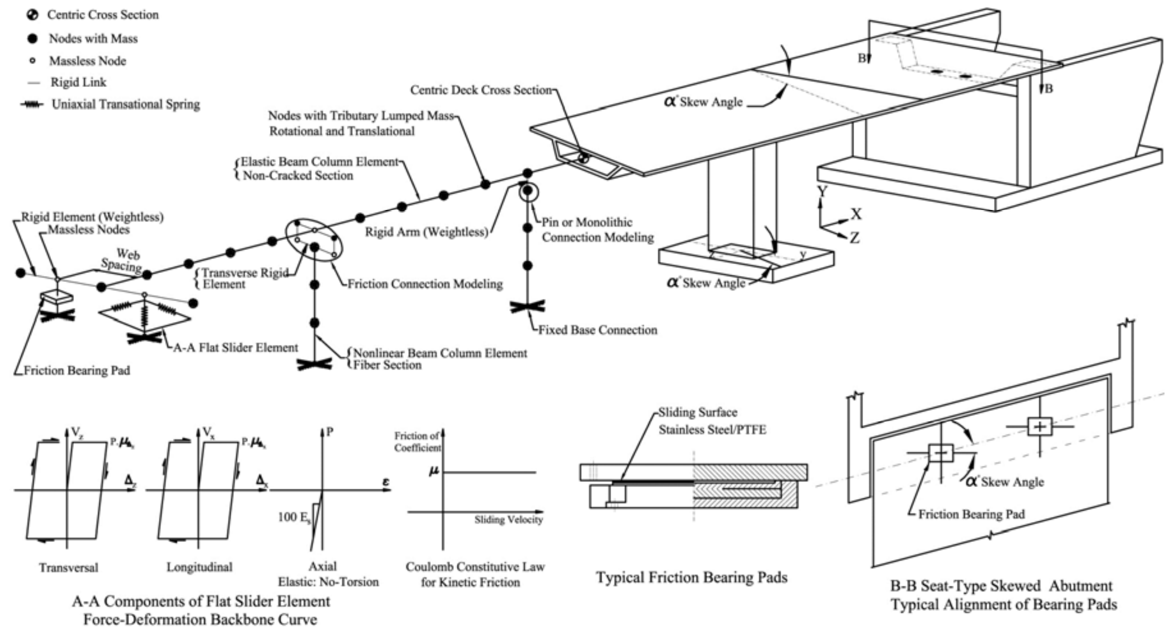

Fig. 6 The generic skewed bridge model, used for non linear time history analysis

3. Connection types

Three different pier-deck connections are applied in the considered skew angles. The schematic description of studied cases is presented in Fig. 5. Both types of monolithic and seat-type pier-deck connections have been already applied in the straight bridge (Casarotti and Pinho 2006, Akbari and Maalek 2010). In the fixed or monolithic connections (M models), the reinforcement bars of the pier are well anchored into the deck. In the seat-type connections, deck simply rests on the bearings (fixed or sliding) and the relative rotation is free between sub- and superstructure. The interior shear keys and restrainers are intended to prevent superstructure from experiencing large displacements. In fact shear keys fail when shear demand exceeds their capacity. The extreme scenarios for seismic behavior of shear keys are: a) fully operational or fixed; b) failed or ineffective. Here, P models are seat-type bridges with fixed bearings and fully operational shear keys (pinned piers). In these connections, relative displacement between pier and deck is totally eliminated and shear forces are transferred by shear keys from superstructure to the substructure. F models stand for seat-type bridges with frictional sliding bearings and no internal shear keys. The sliding bearings have plate interfaces of ploytetrofluoroethylene (PTFE) and stainless steel. It should be noted that the actual behavior of internal shear keys is between the aforementioned scenarios. The role of shear keys would be examined better by modeling two extreme states.

4. 3-Dimensional modeling of skewed bridges

Numerical analyses are carried out in the OpenSees (2008) finite element package. The package has numerous options for material and element modeling. It can execute scripted repetitive nonlinear time-history analyses and process the results. In this regard, the process of earthquake engineering studies could be expedited considerably in the OpenSees. The accuracy of the software and modeling techniques used in this study, have been demonstrated and verified by a large scale test conducted by Sadrossadat and Saiidi (2007) on a four span bridge in University of Nevada Reno. Fig. 6 shows a typical finite element spine model of the representative skewed bridge, used in the simulations. Verified and validated modeling approaches are applied in this study based on previous works (Aviram *et al*. 2008, Casarotti and Pinho 2006). Details of modeling process are provided in the following.

4.1 Modeling of the superstructure

The pre-stressed box girder deck is modeled using five linear elastic-beam-column elements with equal lengths in each span. Table 1 presents the geometrical non-cracked characteristics of the deck. In this table A is cross sectional area; I_z and I_y are moments of inertia about horizontal and vertical axes of the section, respectively; J is torsional constant; E is Young's modulus (25 GPa); and G is shear modulus (10 GPa). The deck element is modeled at the height of its center of gravity, 1.51 m above the pier, and connected to the top of the pier by a rigid element (Fig. 6). The distributed mass of deck elements is about 20.2 ton/m, considering the thickness of asphalt overlay (about 10 cm) and the specific weight of concrete and asphalt (25 and 20 kN/m^3, respectively). The translational and rotational nodal masses are computed and assigned based on the above mentioned values.

4.2 Modeling and verifying of the pier bents

Regarding the combined seismic behavior of piers in skewed bridges, a modeling technique should be applied to account for the interaction between moments and axial load. The integrated fiber section modeling by nonlinear beam-column elements can inherently accounts for geometric nonlinearity and material inelasticity. The piers are divided into three force based nonlinear-beam-column elements with equal lengths. Each element consists of three integration points with fiber sections. Steel02 and Concrete02 are used for modeling uniaxial stress-strain relationship of the fibers, according to the constitutive laws of Menegotto and Pinto (1973) and Mander (1988),

Table 1 Elastic properties of deck cross section

EA(10^7 kN)	EI$_y$(10^7 kN.m^2)	EI$_z$(10^7 kN.m^2)	GJ (10^7 kN.m^2)
17.4	13.43	221.13	13.06

respectively. In order to obtain shear and torsional demands of the piers in OpenSees (2008), their behavior model should be aggregated with the fiber section. The torsion in single bent piers is compatibility type (Priestley *et al.* 1996). For accurate estimation of torsional demand, Caltrans (2010) has recommended to reduce the torsional stiffness of piers to $0.2J_c$, concerning the initial cracking. Torsional and shear behaviors are modeled by uniaxial elastic materials. In this way of modeling, the occurrence of shear failure in the piers should be investigated manually by comparing shear demands and capacity. The fiber cross section, uniaxial material models, shear and torsion behavior models are shown in Fig. 7.

Several experimental and numerical studies have been conducted on the selected bridge (Pinto *et al.* 1996, Cassaroti and pinho 2006). The adequacy and accuracy of modeling assumptions of this study have been verified by the authors (Attarchain *et al.* 2013). Fig. 8 presents the cyclic relation between base shear and displacement at the top of the scaled pier (1:2.5) with a total

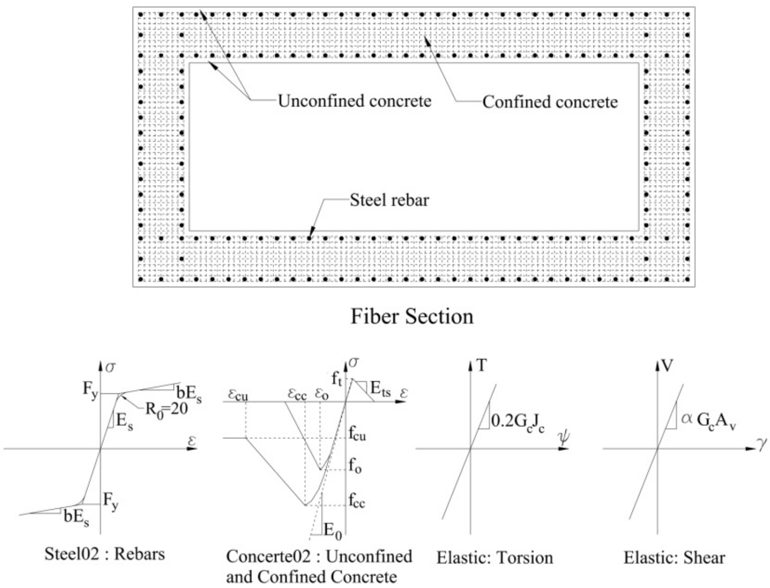

Fig. 7 Pier fiber cross section and applied constitutive rules

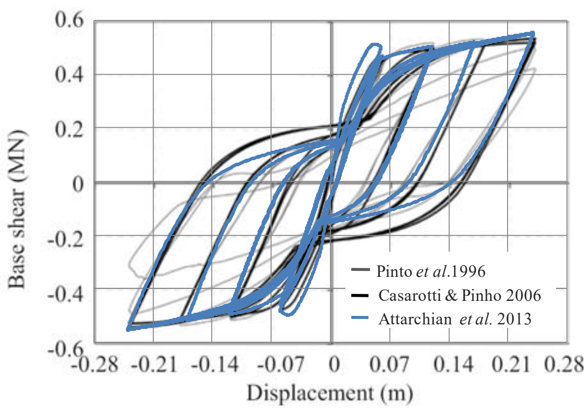

Fig. 8 Comparing cyclic experimental and numerical results of a 1:2.5 scaled pier (Attarchain *et al.* 2013)

height of 8.4 m. Based on this figure, the present numerical model pretty agrees with the experimental results of Pinto *et al*. (1996). Besides, the numerical model prepared by Attarchain *et al*. (2013), can satisfactory capture pinching behavior of the specimens, comparing with numerical results of Casarotti and Pinho (2006).

4.3 Modeling of the connections

The default connection between elements in OpenSees is fixed type. This connection is applied in M models. In order to model seat-type pier-deck connections, an extra node is defined with the same coordination at top of the pier. In P models, the extra node and the node at the top of the pier are constrained to each other only in the transitional degrees of freedom. In this way of modeling, the relative displacement is eliminated, but relative rotation is allowed between deck and pier. In F models, sliding bearing is modeled by flat slider bearing element, a zero length element between the extra node and the bottom node of the rigid element. According to OpenSees command manual (2008), the flat slider bearing element has coupled friction properties for shear along both directions, and no-tension uniaxial material for axial behavior in order to capture uplift behavior. Fig. 6 presents the typical friction sliding bearing and its force-deformation backbone curves. Shear resistance depends on the axial compression load and friction coefficient. Friction is modeled by Coulomb Friction model in which variation of kinetic friction coefficient is constant against sliding velocity. For seismic displacement rates, friction coefficient of (PTFE) bearings is predicted around 15% (Priestley *et al*. 1996).

4.4 Modeling of boundary conditions

Two ends of the deck are modeled by a rigid element to better describe the displacement and rotation of deck in the boundaries, Fig. 6. It is obvious that modeling the behavior of abutments and shear keys would affect the seismic behavior of the bridge. The main objective of this research is to study the effect of different pier-deck connections on the seismic behavior of skewed bridges. Parameters under investigation in this study are a) different pier-deck connections, b) skew angles. It would be complicated to determine the share values of each parameter by modeling the behavior of boundaries. Therefore, the interaction between abutment and bridge is ignored in this research.

5. Dynamic characteristics of the bridges

Eigen value analysis has been carried out prior to nonlinear time history analysis to obtain the modal properties of the models. The obtained results have been compared with dynamic characteristics of the reference bridge. Akbari and Maalek (2010) have reported the modal analysis results for the straight bridge with monolithic pier-deck connections (B111). Characteristics of B111 model are compared with those of M0 and presented in Table 2. In order to verify the dynamic properties of the presented model, the boundary conditions in abutments are assigned along with the assumptions of Akbari and Maalek (2010). According to Table 2, no significant difference is seen between the modal properties of B111 and those of M0 models. This fact confirms the adequacy of generated model for dynamic analysis. Tables 3-5 present the natural periods and dominant mode shapes of generated models. Long. and Trans. in tables stand for longitudinal and transversal modes, respectively. For all connection types, the first dominant mode

Table 2 Modal properties of the first three transversal modes for B111 and M0 model

Akbari and Maalek (2010)-B111		Present Study- M0 model	
T (sec)	M *	T (sec)	M *
0.216	75.6%	0.213	77%
0.188	0%	0.198	0%
0.157	8%	0.171	9.7%

Table 3 Modal analysis results in M models

M0		M15		M30		M45		M60	
Mode	T(sec)	Mode	T(sec)	Mode	T(sec)	Mode	T(sec)	Mode	T(sec)
Torsional	0.427	Torsional	0.423	Torsional	0.413	Torsional	0.394	Torsional	0.378
Trans.	0.216	Trans.-Long.	0.231	Trans.-Long.	0.253	Trans.-Long.	0.280	Trans.	0.328
Long.	0.215	Trans.	0.214	Trans.	0.221	Trans.	0.233	Trans.	0.272
Trans.	0.212	Trans.-Long.	0.205	Trans.	0.203	Trans.-Long.	0.204	Trans.-Long.	0.211
Trans.	0.199	Trans.-Long.	0.198	Long.	0.192	Long.	0.185	Long.	0.177

Table 4 Modal analysis results in P models

P0		P15		P30		P45		P60	
Mode	T(sec)	Mode	T(sec)	Mode	T(sec)	Mode	T(sec)	Mode	T(sec)
Torsional	0.522	Torsional	0.521	Torsional	0.515	Torsional	0.504	Torsional	0.5
Trans.	0.295	Trans.	0.304	Trans.-Long.	0.320	Trans.-Long.	0.334	Trans.	0.337
Long.	0.250	Long.	0.241	Trans.	0.226	Trans.	0.237	Trans.	0.254
Trans.	0.218	Trans.	0.220	Long.	0.224	Long.- Trans.	0.208	Trans.-Long.	0.210
Trans.	0.201	Trans.	0.202	Trans.-Long.	0.204	Trans.-Long.	0.205	Long.	0.188

Table 5 Modal analysis results in F models

F0		F15		F30		F45		F60	
Mode	T(sec)	Mode	T(sec)	Mode	T(sec)	Mode	T(sec)	Mode	T(sec)
Torsional	0.524	Torsional	0.522	Torsional	0.518	Torsional	0.513	Torsional	0.509
Trans.	0.335	Trans.	0.340	Trans.	0.351	Trans.	0.357	Trans.	0.442
Long.	0.267	Long.	0.261	Trans.	0.262	Trans.	0.274	Trans.	0.287
Trans.	0.254	Trans.	0.256	Long.	0.250	Long.	0.236	Long.	0.224
Trans.	0.218	Trans.	0.219	Trans.	0.221	Trans.	0.223	Trans.	0.223

shape is torsional due to the lack of restrainers in the boundaries. Indeed, straight bridges have similar decoupled mode patterns regardless of the connection types. However, in the skewed bridges mode shapes are coupled including both transversal and longitudinal movements. For all cases as the skew angle increases, the transversal modes become more dominant and the natural period of the system is elongated. The mode shapes are not coupled in the F models due to the lack of internal restrainers. Concerning the connection types, the flexibility of the bridges increases as

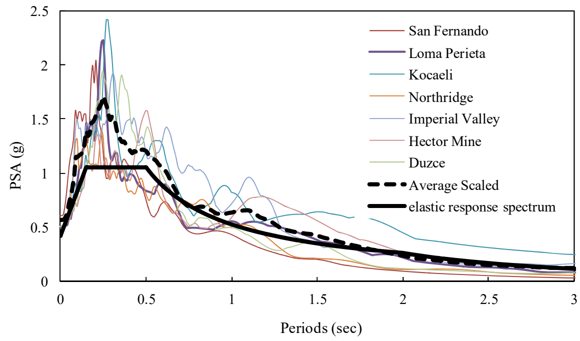

Fig. 9 Acceleration Response Spectrum (ARS) of scaled records beside elastic design spectrum (soil B, a_g=0.35 g)

Table 6 The characteristics of strong ground motions

EQ. Name	Year	Station	M	D(km)
San Fernando	1971	Lake Hughes	6.6	25.1
Loma Prieta	1989	Gilroy Array	6.9	18.3
Kocaeli, Turkey	1999	Izmit	7.5	7.2
Northridge	1994	Wonderland	6.7	20.3
Imperial Valley	1979	Cerro Prieto	6.5	15.2
Hector Mine	1999	Hector	7.1	11.7
Duzce, Turkey	1999	Lamont	7.1	8

the rigidity of the sub- and superstructure connection decreases.

6. Ground motion records and strike angle

Seven independent pairs of horizontal ground motions have been selected for non-linear time history analysis. These ground motions are chosen from the second set of broadband motions introduced by Baker *et al*. (2011) on the rocky sites. The relevant response spectra are in accordance with the median and log standard deviations derived for the strike slip earthquakes of magnitude 7 at 10 km distance. The site V_{s30} has been assumed as 760 m/sec. Characteristics of the ground motions are presented in Table 6. Records are scaled to the elastic design spectrum (type 1) of EC8 (CEN 2004), soil type B, PGA=0.35 g. Records are scaled such that the average value of SRSS spectra of the normalized components does not fall below 1.4 times of the elastic design spectrum for periods within 0.1 to 0.5 seconds. The resulted scaling factor is 0.5 g, Fig. 9.

Strong ground motion records are applied along and perpendicular to the bridge alignment, respectively. As shown in Fig. 3, major or primary and minor or secondary horizontal components of the ground motion are applied along the longitudinal and transversal directions of the bridge, respectively. OpenSees (2008) considers the excitations only along the global axes system *X*-*Y*-*Z* (Fig. 3). Therefore, the records are derived for each skew angle along the global directions (*X*,*Z*), according to Somerville (2002) as follows

$$X = L \cdot Cos\,(\alpha) - T \cdot Sin\,(\alpha) \tag{1}$$

$$Z = L \cdot Sin\,(\alpha) + T \cdot Cos\,(\alpha) \tag{2}$$

7. Nonlinear time history analysis

Bidirectional nonlinear time history analyses have been carried out with seven input ground motions, on the introduced models for different skew angles (0°, 15°, 30°, 45° and 60°), according to EC8 (CEN 2004). Various global, intermediate and local engineering demand parameters, (EDP) have been defined by Mackie and Stojadinović (2005). Several EDPs have been selected in order to compare the overall behavior of bridge models plus the performance of structural components. Transversal displacement and rotational demand in the deck can depict the probability of deck collapse. The performance of structural system is investigated by monitoring the displacement ductility and force demands in the piers, bearings and connections. The cross-sectional moment curvature loops are derived, in order to investigate the effect of combined loading plus the local behavior of plastic hinges.

It should be noted that demand refers to the maximum absolute value of the time history responses. The mean and one standard deviation of the selected EDPs are calculated to evaluate the seismic performances. The results have been discussed in the following, considering the effect of skew angle and different connections.

7.1 Displacement demand of the deck

Mean transversal displacement demand of the deck Δ_d is shown along the bridge, Fig. 10. It should be mentioned that the standard deviation values are 6-14% for the transversal displacement demand results. Generally, it is anticipated that Δ_d decreases as the rigidity of the pier-deck connection increases. Accordingly, the smallest and largest displacement demands belong to M and F models, respectively, Fig. 10. Variation of Δ_d along the bridge is similar to a wide W, due to

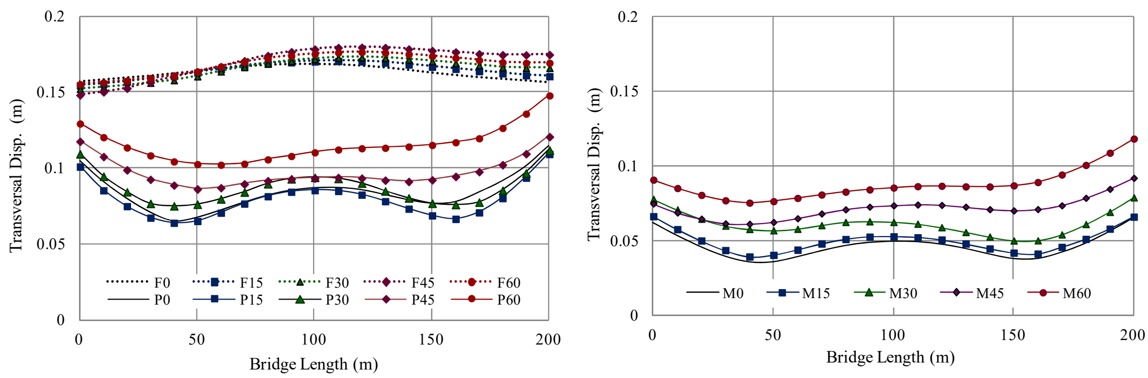

(a) F and P models (b) M models

Fig. 10 Mean transversal displacement demand along the bridge

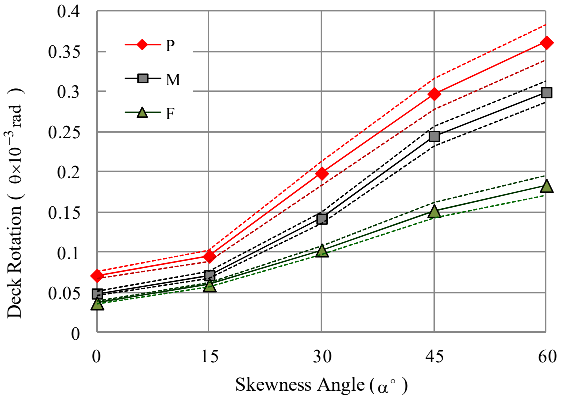

Fig. 11 Mean and one standard deviation of rotational demand in the deck

the elimination of shear keys in the abutments during the modeling. Based on Fig. 10, the displacement demand (Δ_d) is quite similar in P and M models, for skew angles less than 30°. However, for the skew angles higher than 30° the transversal displacement demand in the P models increases steeply with the skew angle. In the F models, the deck has moved considerably over the bearings like a solid element, due to the lack of internal shear keys, Fig. 10(a). Therefore, deck collapse is quite probable in seat-type skewed bridges while shear keys are ineffective. Internal shear keys play a significant role in controlling displacement demand of the deck, regarding Δ_d of P and F models, Fig. 10(a). Based on the results presented in Fig. 10, it is reasonable to apply seat-type connections in bridges with relatively small skew angles (<30°). In this case shear keys should be designed to be fully operational. For bridges with skew angles higher than 30°, using monolithic pier-deck connections can diminish and control the displacement demand of the deck.

7.2 Rotational demand of the deck

Fig. 11 shows mean and one standard deviation of the rotational demand in the deck. According to this figure, rotational demand increases in all models as the skew angle increases. The rate of this increase steepens in skew angles over 15°. Based on this figure the rotational demand value is up to 30% lower in M models due to the rigidity of pier-deck connection, comparing to that of P models. The rotational demand has the lowest value in the F models due to the uniform solid movement of the deck over the bearings. Comparing the results obtained from P and M models, it can be concluded that the deck can experience considerable rotations regardless the effectiveness of shear keys. Based on the rotational demand values of the deck in P models, the shear keys are prone to fail in the higher skew angles. The deck collapse probability should be evaluated by combining transversal displacement and rotational demands. In this regard, deck collapse is quite probable in the highly skewed bridges (>30°) with seat-type connections. Consequently, monolithic pier-deck connections are more appropriate for highly skewed bridges.

7.3 Deformation demand on the substructure system

Mean displacement ductility demand $\mu_\Delta=\Delta_d/\Delta_{ye}$ is computed along both local axes of the piers.

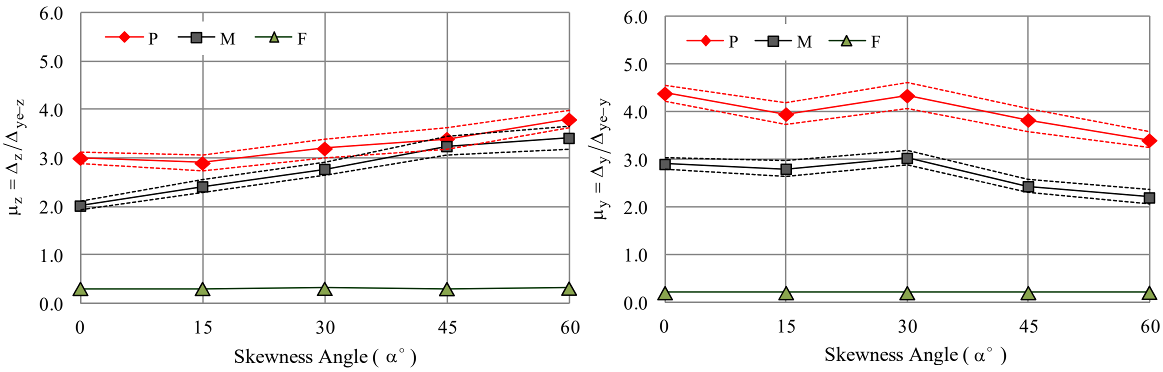

(a) μ_Δ along local *z* axis (b) μ_Δ along local *y* axis

Fig. 12 Mean and one standard deviation of displacement ductility demand in the piers

Regarding no irregularity in the height and configuration of the piers along the bridge, the trend of displacement ductility demand is quite similar in all piers. Therefore, only the results of the middle piers are presented in Fig. 12. The relative yield displacement, between the critical section and the point of contra flexure, could be approximated by $\Delta_{ye} = C_1 \phi_{ye} (H + L_{SP})^2$, according to Priestley (2007) and Caltrans (2010). In this formula, C_1 is a constant, dependent on the boundary conditions; L_{SP} is strain penetration length, over which the curvature can be considered equal to the base curvature; and ϕ_{ye} is yield curvature. Δ_{ye} is computed for each pier, considering the type of boundary condition, based on the constants and formula presented by Priestley (2007). Based on Fig. 12 no ductility demand is needed in the piers of F models. In these models, with sliding bearings and ineffective shear keys, the deck moves over bearings like a solid element and the piers remain totally elastic. Ductility demand is relatively greater in the piers of P models, comparing to that of M models, due to the concentration of plastic deformation at the bottom of piers, Fig. 12. Particularly μ_Δ of pinned piers along the minor local axis *y* is considerably higher than that in fixed piers where monolithically connected piers are in a double curvature pattern. The variation of ductility demands with the skew angle is contrariwise along the local axes of *z* and *y*, Fig. 12. That is because of the variation of dominant axis with the skew angle. The ductility demand in the piers increases along the major local axis *z* as the skew angle increases; due to the dominating role of *z* axis in sustaining movements.

7.4 Axial-flexural and shear demand in the piers

No significant difference is seen between the trend of force demands in the middle and side piers. Demand ratios at the base of the left piers are shown in Fig. 13. As mentioned earlier *y* and *z* are the local axes of the pier section. Shear ratio R_V is obtained from dividing shear demand V_d by nominal shear capacity of the section V_n Shear capacity of the piers is estimated according to Caltrans method, established upon Priestley model (1994). Based on Fig. 13 (a, b) the trend of shear ratios is contrariwise along the local axes of *z* and *y*. The shear ratio demand along major *z* axis R_{Vz} increases with the skew angle, Fig. 13(a). This is probably due to the dominating role of *z* axis in sustaining the transversal demands. Based on Fig. 13(a), R_{Vz} in fixed piers is higher than those in pinned piers, and increases up to 80% of the nominal capacity. The shear ratio demands

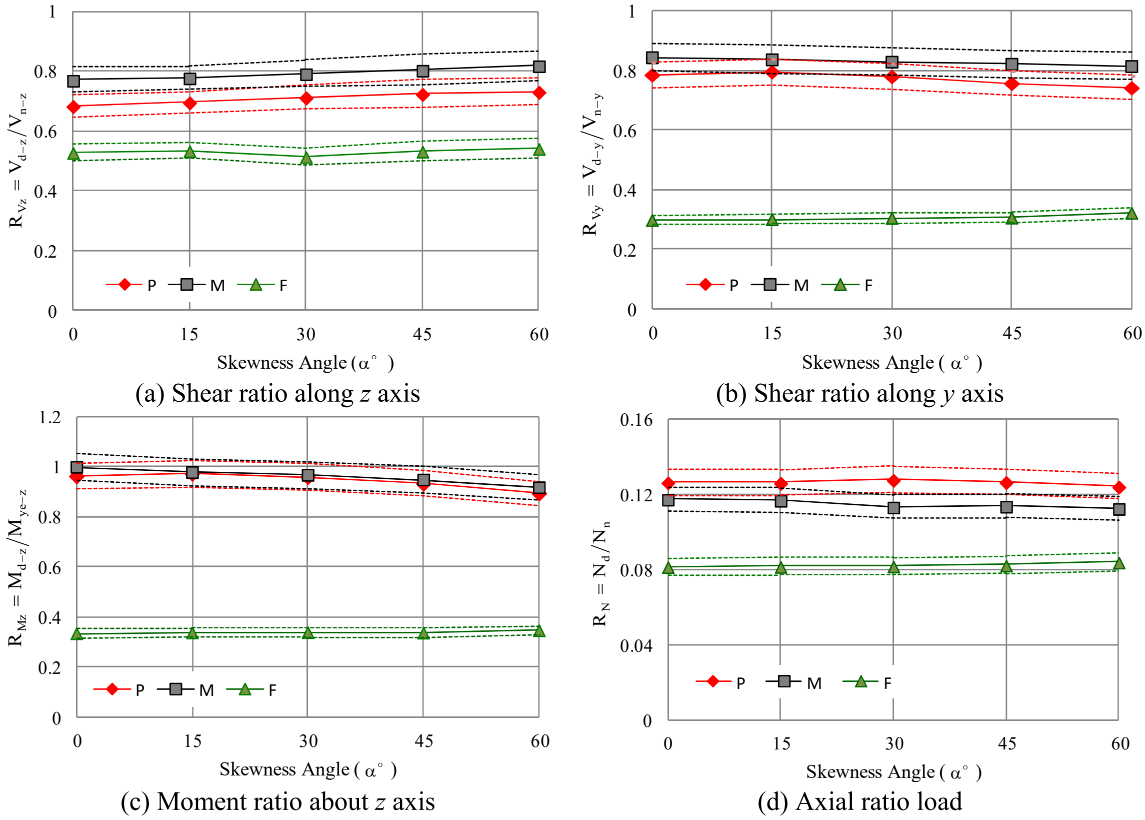

(a) Shear ratio along *z* axis
(b) Shear ratio along *y* axis
(c) Moment ratio about *z* axis
(d) Axial ratio load

Fig. 13 Mean and one standard deviation of the demand ratios at the base of the left piers

along minor *y* axis R_{Vy} slightly decrease with the skew angle, Fig. 13(b). Despite fixity provided in modeling of monolithic piers, fixed piers are in single curvature pattern along *y* axes, similar to pinned piers. Therefore, as shown in Fig. 13(b) the shear demand along y axis (R_{Vy}) is quite similar in pinned and fixed piers. In F models shear demand is limited to the friction force transmitted by bearings and thereby quite far from the nominal shear strength of the sections. Shear ratio along *z* axis of F models is twice *y* axis due to the rectangular shape of pier section, Fig. 13(a), (b).

Moment ratio about major local axis *z* R_{Mz} is determined through dividing moment demand M_d by yield moment of the section M_{ye}. The yield moment of the section is determined through moment curvature analysis. Based on Fig. 13(c), moment demands at the base of the piers of M and P models have met the yield capacity of the sections. The base section of pier in M and P models have experienced plastic deformations as shown in Fig. 15. According to Fig. 13(c), the piers remain elastic in F models. The axial load ratio R_N is presented in Fig. 13(d). It should be mentioned that the gravity loading is about 7% of nominal axial capacity N_n of the piers. Axial load is approximately in the gravity load range concerning the piers of F models. However, the piers of P and M models are subjected to additional axial seismic demand.

7.5 Torsional demand in the piers with monolithic pier-deck connections

Torsion in single pier bent bridges is induced by compatibility requirements (Priestley *et al.*

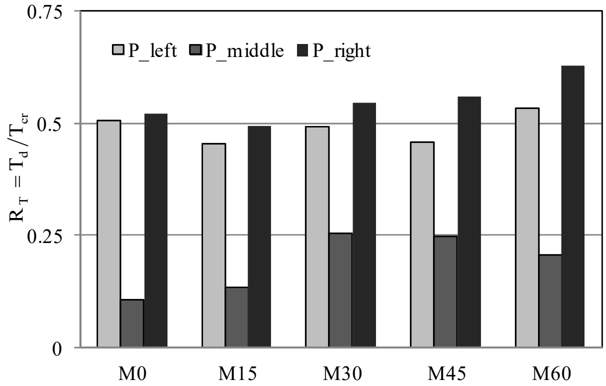

Fig. 14 Mean torsional demand ratios in the piers of M models

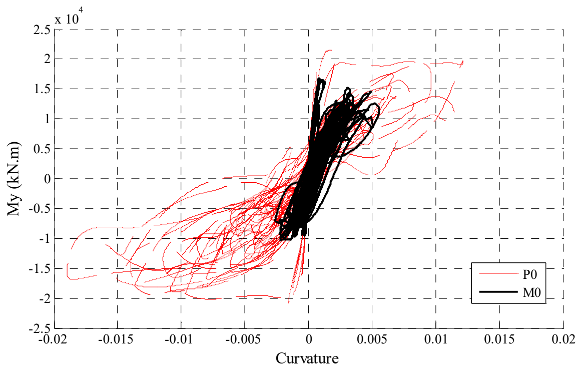

(a) Moment about y axis, straight bridge

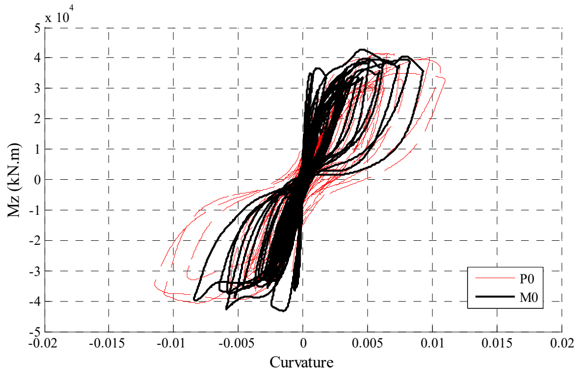

(b) Moment about z axis, straight bridge

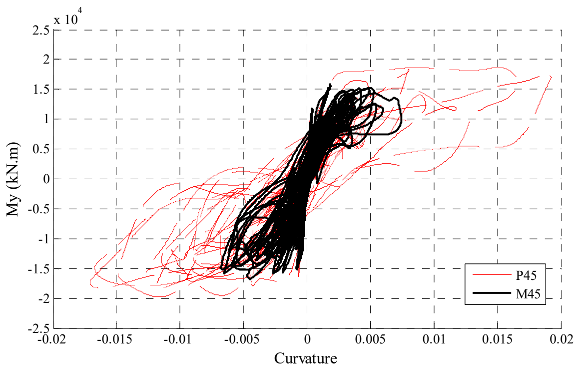

(c) Moment about y axis, 45° skewed bridge

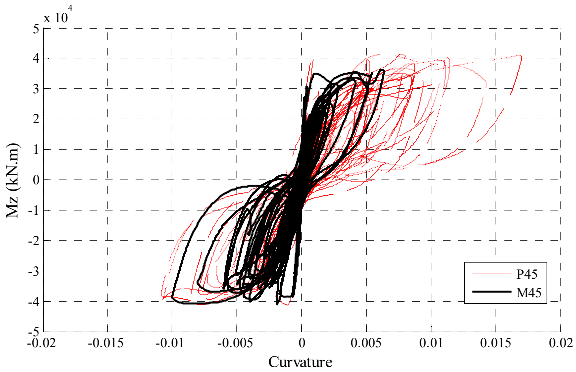

(d) Moment about z axis, 45° skewed bridge

Fig. 15 Moment curvature demand at the base of left pier under Imperial Valley earthquake (1979), P: pinned, M: monolithic

1996). According to EC2 (CEN 2004) when torsion arises from consideration of compatibility, minimum reinforcement should be provided to prevent excessive cracking. In order to estimate the intensity of the probable cracking in the piers, the cracking torque T_{cr} is derived according to AASHTO (2012). Fig. 14 shows the ratio of torsional demand in piers with monolithic pier-deck connections. One standard deviation of the mean torsional demand is about 6-9% in the piers. Torsional ratio R_T is obtained from dividing torsional demand T_d by cracking torque T_{cr} of the section. In the single pier bridges, the torsional stiffness is mainly provided by the side piers. As a result of this, torsional demand is higher in the side piers, comparing to the middle ones. According to Fig. 14, torsional demand increases in piers as the skew angle increases. Further, torsional demand in the side piers is larger than twice torsional demand in the middle piers, Fig. 14.

It should be noted that piers with monolithic pier-deck connections are under combined torsional-flexural loading. According to performance based design method, Caltrans (2010), flexural deformation capacity has an important role in capacity design of bridge piers. According to AASHTO (2012): "If the factored torsional moment is less than one quarter of the factored pure torsional cracking moment, it will cause only a very small reduction in shear capacity or flexural capacity and, hence, can be neglected". Accordingly, effect of torsional demand on flexural and shear capacity cannot be neglected in the side piers with monolithic pier-deck connections, Fig. 14. It is necessary to investigate the effect of torsional demand on the flexural behavior and deformation capacity of the piers. Considering the trend of shear and torsional demand in the fixed piers, shear failure is probable in the side piers of skewed bridges with monolithic pier-deck connections.

7.6 Moment curvature demand in the piers

Moment curvature demand curves are derived for fixed and pinned piers in order to investigate their nonlinear behavior in the plastic hinge regions. The curves shown in Fig. 15 are related to the base section of the left pier under Imperial Valley earthquake (1979). In this figure the inelastic behavior of monolithic (M) and pinned (P) piers have been compared in the straight and 45° skewed bridges. As shown in Fig. 15, investigated hollow rectangular piers suffer from considerable pinching behavior. This observation is consistent with those reported by Qiang *et al.* (2013, 2014) in their experimental and numerical researches on hollow rectangular bridge columns. According to Fig. 15, inelastic curvature demand is significantly higher at the base of piers of P models comparing with that of M models. This fact could be due to the deformation concentration at the bottom of pinned piers. Similar behavior is observed in the moment curvature demand curves of pinned and fixed piers for other ground motions, aren't presented here for the sake of brevity. According to Fig. 15, the plastic deformation demand is higher in the 45° skewed bridges in comparison with that of straight bridges, in both connection types.

7.7 Shear demand in pier-deck connections

The trend of shear demand is similar in middle and side pier-deck connections. Fig. 16 shows mean shear demand in the middle pier-deck connections. For P and F models, mean shear demand in fixed and sliding bearings is reported, respectively. According to section 7.1, providing fixed bearings with effective shear keys is essential for eliminating the possibility of deck collapse. Based on Fig. 16, the value of shear demand in fixed bearings is about 40% higher than those in the sliding bearings. Although 40% more shear demand is considerable, but providing this capacity is inevitable according to findings in 7.1. For skew angles higher than 30°, particularly in pinned pier bridges, displacement and rotational demand of the deck increases (see section 7.1 and 7.2). In this regard, for skew angles higher than 30° applying monolithic pier-deck connection is essential.

Based on Fig. 16, shear demand in monolithic connections increases up to 20% comparing with those in fixed bearings (P models). Moreover, shear demand in the connections is almost the same in all skew angles. Since no extra shear demand is imposed on the monolithic connections regarding the skew angle; applying monolithic connections is sensible in skew angles higher than 30°.

The shear-displacement time histories are derived for the sliding bearings. Fig. 17 shows the shear-displacement time histories of the left and middle bearings in model F15 under Northridge earthquake (1994). The movements along z and y directions are presented in the left and right sides of the figure, respectively. Shear-displacement behavior of the bearings is similar to that of the flat slider bearing element, defined in 4.3. Residual displacement of the bearings and shear force level can be observed in the figure as well. As can be seen in Fig. 16, shear demand subjected to the substructure is limited to friction force of sliders. Friction mechanism and hysteresis behavior developed in flat sliders dissipates considerable amount of kinetic energy and protects substructure system in comparison to monolithic and pinned pier-deck connection types. However, this is achieved at the cost of 0.1 and 0.12 (m) residual displacement in the y and z directions, respectively.

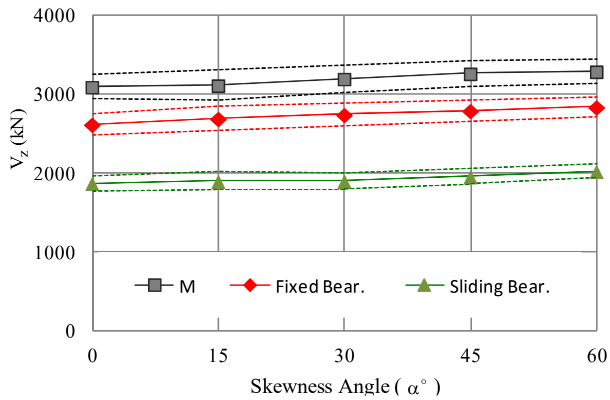

Fig. 16 Mean and one standard deviation of shear demand along z axis in the middle pier-deck connections

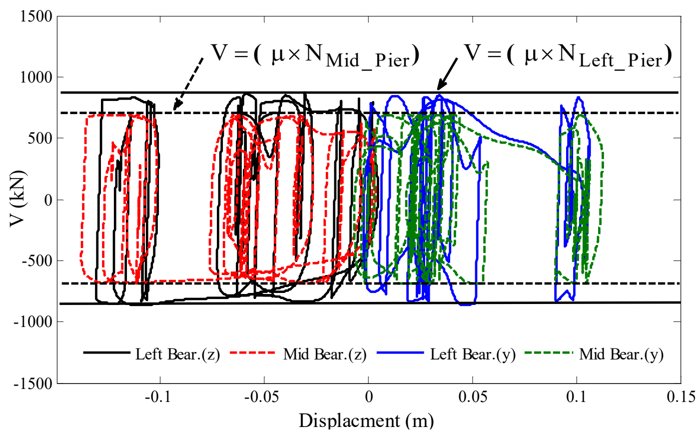

Fig. 17 Shear-displacement curve of the left and middle pier bearings under the Northridge earthquake (1994), F15 model

8. Conclusions

In this study a four span continuous deck bridge with single pier bents has been modeled and verified. Parameters under investigation in this study are a) different pier-deck connections, b) skew angles. Three different pier-deck connection types are considered. The skew angles vary from 0° to 60°. In order to determine the pure influence of varying parameters, the interaction between abutment and bridge is ignored. Seismic performance of the bridges is investigated conducting bidirectional nonlinear time history analysis in OpenSees. Seven independent pairs of horizontal ground motions have been selected and scaled to the elastic design spectrum (type 1) of EC8 (CEN 2004), soil type B, PGA=0.35 g. The mean value of the responses is derived and evaluated. Several global and intermediate engineering demand parameters (EDP) have been selected for studying the overall behavior of the bridges plus the structural components. The obtained results are briefly summarized as follows:

• The movement could be quite controlled in the deck of seat-type bridges with skew angles up to 30°, if shear keys are effective and function properly (as assumed in P models). In the larger skew angles (>30°), the displacement demand increases considerably in the deck of P models; consequently, the probability of deck collapse would be serious. Therefore, applying monolithic pier-deck connections is indispensable for the bridges with skew angles greater than 30 degrees.

• While shear keys are not effective in seat-type bridges (as assumed in F models) the deck undergoes considerable displacement demand and bearings experience residual displacement. Deck collapse is quite probable in F models.

• In all models the rotational demand increases with the skew angle. As opposed to P models, the rotational demand decreases up to 30% in the M models by providing rigidity in the pier-deck connections. Therefore, applying monolithic pier-deck connections is more sensible in the highly skewed bridges (>30°).

• The displacement ductility demand in pinned piers (P models) is relatively greater than those in fixed piers (M models). This is due to the concentration of plastic deformation at the bottom of pinned piers. In the absence of shear keys in F models, the piers remain elastic and their shear demands are limited to the friction force transmitted by sliding bearings.

• The torsional demand in the side piers with monolithic pier-deck connections is about half of the cracking torque. Moreover, its value increases as the skew angle increases.

• Piers of skewed bridges with monolithic pier-deck connections experience combined flexural and torsional loading. Regarding to the obtained torsional demand rates, it is necessary to investigate the effect of torsional demand on the flexural behavior and deformation capacity of the piers.

Acknowledgments

The research described in this paper was financially supported by the International Institute of Earthquake Engineering and Seismology (IIEES) under the Grant No. 7729.

References

AASHTO (2012), *AASHTO LRFD Bridge Design Specification*, American Association of State Highway and Transportation Officials.

Akbari, R. and Maalek, Sh. (2010), "Adequacy of the seismic analysis method for single-column-bent viaducts considering regularity and higher modes effects", *J. Vib. Control*, **16**(6), 827-852.

Attarchain, N., Kalantari, A. and Moghaddam, A.S. (2013), "Cyclic behavior modeling of rectangular RC bridge piers using OpenSees", *Proceedings of the: 4th ECCOMAS Thematic Conference on Computational Methods in Structural Dynamics and Earthquake Engineering, COMPDYN 2013*. Kos Island, Greece.

Aviram, A., Mackie, K.R. and Stojadinović, B. (2008), *Guidelines for Nonlinear Analysis of Bridge Structures in California*, PEER Report. 2008/03.

Baker, J.W., Lin, T., Shahi, S.K. and Jayaram, N. (2011), *New Ground Motion Selection Procedures and Selected Motions for the PEER Transportation Research Program*, PEER Report 2011/03.

Bhagwat, M., Sasmal, S., Novak, B. and Upadhyay, A. (2011), "Investigations on seismic response of two span cable-stayed bridges", *Earthq. Struct.*, **2**(4), 337-356.

Caltrans SDC, (2010), *Caltrans seismic design criteria version 1.6*, California Department of Transportation, Sacramento.

Casarotti, Ch. and Pinho, R. (2006), "Seismic response of continuous span bridges through fiber-based finite element analysis", *Earthq. Eng. Eng. Vib.*, **5**(1), 119-131.

CEN European Committee for Normalization, Eurocode 8 (2004), *Design of Structures for Earthquake Resistance-Part 1, general rules, seismic actions and rules for buildings*, EN 1998-1.

CEN European Committee for Normalization, Eurocode 2 (2004), *Design of concrete structures-Part 1-1, general rules and rules for buildings*, EN 1992-1-1.

CEN European Committee for Normalization, Eurocode 8 (2005), *Design of Structures for Earthquake Resistance-Part 2, Bridges*, EN 1998-2.

Elnashai, A.S., Gencturk, B., Kwon, O.S., Al-Qadi, I., Hashash, Y., Roesler, J.R., Kim, S.J., Jeong, S.H., Dukes, J. and Valdivia, A. (2010), "The Maule (Chile) Earthquake of February 27, 2010, consequence assessment and case studies", MAE Center, Report No. 10-04, 208.

Ghobarah, A.A. and Tso, W.K. (1974), "Seismic analysis of skewed highway bridges with intermediate supports", *Earthq. Eng. Struct. Dyn.*, **2**(3), 235-248.

Ijima, K., Obiya, H., Aramaki, G. and Kawasaki, N. (2001) "A study on preventing the fall of skew and curved bridge decks by using rubber bearings", *Struct. Eng. Mech.*, **12**(4), 347-362.

Isakovi´C, T., Lazaro, M. and Fischinger, M. (2008), "Applicability of pushover methods for the seismic analysis of single column bent viaducts", *Earthq. Eng. Struct. Dyn.*, **37**(8), 1185-1202.

Kalantari, A. and Amjadian, M. (2010), "An approximate method for dynamic analysis of skewed highway bridges with continuous rigid deck", *Eng. Struct.*, **32**(9), 2850-2860.

Kappos, A.J., Manolis, G.D. and Moschonas, I.F. (2002), "Seismic Assessment and design of R/C bridges with irregular configuration, including SSI effects", *Eng. Struct.*, **24**(10), 1337-1348.

Kaviani, P., Zareian, F. and Taciroglu, E. (2012), "Seismic behavior of reinforced concrete bridges with skew-angled seat-type abutments", *Eng. Struct.*, **45**, 137-150.

Kawashima, K., Takahashi, Y., Ge, H., Wu, Z. and Zhang, J. (2009), "Reconnaissance report on damage of bridges in 2008 Wenchuan, China, Earthquake", *J. Earthq. Eng.*, **13**(7), 965-996.

Mackie, K.R. and Stojadinović, B. (2005), *Fragility Basis for California Highway Overpass Bridge Seismic Decision Making*, PEER Report. 2005/12.

Mander, J.B., Priestley, M.J.N. and Park, R. (1988), "Theoretical stress-strain model for confined concrete", *J. Struct. Eng*., ASCE, **114**(8), 1804-1826.

Menegotto, M. and Pinto, P.E. (1973), "Method of analysis for cyclically loaded R.C. plane frames including changes in geometry and non-elastic behavior of elements under combined normal force and bending", *Symposium on the Resistance and Ultimate Deformability of structures Acted on by Well Defined Repeated Loads*, International Association for Bridge and Structural Engineering, Zurich, Switzerland. Lisbon: IABSE Report, Vol.13, Final Report, 15-22.

Meng, J.Y. and Lui, E.M. (2000), "Seismic analysis and assessment of a skew highway bridge", *Eng. Struct.*, **22**(11), 1433-1452.

Mohti, A.A. and Pekcan, G. (2008), "Seismic response of skewed RC box-girder bridges", *Earthq. Eng. Eng.*

Vib., **7**(4), 415-426.

Olmos, B.A. and Roesset, J.M. (2010), "Effects of the nonlinear behavior of lead-rubber bearings on the seismic response of bridges", *Earthq. Struct.*, **1**(2), 215-230.

OpenSees (2008), OpenSees Development Team, *Open System for Earthquake Engineering Simulations,* Version 2.3.0. Available from: http://opensees.berkeley.edu.

Pinto, A.V., Verzeletti, G., Pegon, P., Magonetto, G., Negro, P. and Guedes, J. (1996), *Pseudo-Dynamic and shaking table tests on RC bridges* ECOEST-PrEC8, Report No.5, Brussels.

Priestley, M.J.N., Calvi, G.M. and Kowalsky, M.J. (2007), *Displacement-Based Seismic Design of Structures*, IUSS PRESS, Pavia, Italy.

Priestley, M.J.N., Seible, F. and Calvi, G.M. (1996), *Seismic Design and Retrofit of Bridges*, New York, NY, Wiley.

Priestley, M.J.N., Verma, R. and Xiao, Y. (1994), "Seismic shear strength of reinforced concrete columns", *J. Struct. Eng*., ASCE, **120**(8), 2310-2329.

Qiang, H., Xiuli, D., Zhou, Y. and Lee, G.C. (2013), "Experimental study of hollow rectangular bridge column performance under vertical and cyclically bilateral loads", *Earthq. Eng. Eng. Vib.*, **12**(3), 433-445.

Qiang, H., Yulong, Z., Xiuli, D., Chao, H. and George, C.L. (2014), "Experimental and numerical studies on seismic performance of hollow RC bridge columns", *Earthq. Struct.*, **7**(3), 251-265.

Ramanathan, K., Jeon, J.S., Zakeri, B., DesRoches, R. and Padgett, J.E. (2015), "Seismic response prediction and modeling considerations for curved and skewed concrete box-girder bridges", *Earthq. Struct.*, **9**(6), 1153-1179.

Sadrossadat, Z.M. and Saiidi, S. (2007), *Pre-test Analytical Studies of NEESR-SG 4-Span Bridge Model Using OpenSees*. Report No. CCEER-07-3, Reno Nevada.

Somerville, P.G. (2002), "Characterizing near fault ground motion for the design and evaluation of bridges", *Proceedings of the Third National Seismic Conference and Workshop on Bridges and Highways*, Available from: http://peer.berkeley.edu/research/peertestbeds/Hbt/PaperonNearFaultGroundMotion.pdf.

Yen, Ph., Chen, G., Yashinsky, M., Hashash, Y., Holub, C., Wang, K. and Guo, X. (2011a), *China Earthquake Reconnaissance Report: Performance of Transportation Structures During the May 12, 2008, M7.9 Wenchuan Earthquake*. The Federal Highway Administration, Publication No. FHWA-HRT-11-029 Oct, 54.

Yen, Ph., Chen, G., Buckle, I., Allen, T., Alzamora, D., Jeffrey, G. and Aria, J.G. (2011b), *Post earthquake Reconnaissance Report on Transportation Infrastructure Impact of the February 27, 2010, Offshore Maule Earthquake in Chile*, The Federal Highway Administration, Publication No. FHWA-HRT-11-030 Oct, 218.

Zhao, B. and Taucer, F. (2010), "Performance of infrastructure during the May 12, 2008 Wenchuan earthquake in China", *J. Earthq. Eng.*, **14**(4), 578-600.

Zhiqiang, W. and Lee, G.C. (2009), "A comparative study of bridge damage due to the Wenchuan, Northridge, Loma Prieta and San Fernando earthquakes", *Earthq. Eng. Eng. Vib.*, **8**(2), 251-261.

SA